



MINI REVIEW

Synthetic Fluorometric and Colorimetric Sensors for Identification of Fluoride Anion: A Short Review

SUPRIYA DUTTA¹ and ANIMESH SAHANA^{*,2}

Department of Chemistry, Nistarini College, Purulia-723101, India

*Corresponding author: E-mail: sahana.animesh@gmail.com

Received: 13 March 2024;

Accepted: 13 April 2024;

Published online: 29 June 2024;

AJC-21661

Over two decades of research in fluoride ion detection has been an intriguing field and many papers have been published enriching the possibilities of fluoride ion detection in even nano molar concentration levels. However, few reviews have been published, critically analyzing the design strategies, especially to detect fluoride ions in aqueous and real samples. About 21 colorimetric sensors and fluorescent probes, published during 1999 to 2014 have been covered to analyze their design strategies, speed of detection, limit of detection and their applicability in real samples and in aqueous medium. The fundamental principles can be broadly classified into 5 categories namely Si-O bond cleavage, B-F monomer formation, deprotonation of amide hydrogen, Si-F bond formation and Sb-F bond formations which enable fluoride ion detection. Variations in the organic substituents attached to the Si-O bond, B-F monomer and amide groups is the key to the efficacy of the sensor. Optimization of applicability of the sensors in aqueous solvents *vis-a-vis* maintaining the sensitivity, range of detection, speed of detection, both quantitatively and qualitatively are a challenge. This review aims to present a comprehensive and critically analyzed discussion of the published probes, which will encourage further research in this field.

Keywords: Fluoride detection, Colorimetric sensors, Fluorometric sensors, Si-O bond cleavage, N-H deprotonation.

INTRODUCTION

Sensing of fluoride in real samples as well as samples dissolved in water has been a challenge and designing of fluorogenic and chromogenic sensors have ever since gained intense attraction because of their fast response time, sensitivity, anion specific response and their ease of usage [1-6]. Apart from the fluorometric measurement, naked-eye change of colour has been advantageous for instant detection of fluoride ion. With the help of such probes, analytes can be visualized and monitored quantitatively in living cells microscopically. Initial research was typically based on molecular recognition and host-guest interaction [7]. Naturally, these probes operated in a reversible manner. With time, self-immolated fluorescent probes have been designed for better detection, both qualitatively and quantitatively [8,9]. Inspired from anion binding proteins found in nature, hydrogen-bonded bases like amide, urea, indole, pyrrole, guanidium, *etc.*, fluorescent probes have been synthesized that essentially bind fluoride through hydrogen

bonding [10-16]. Since the basic principles lies in the deprotonation of amide hydrogen of amide linkage, cleavage of silicon-oxygen bond or B-F-B bonds, fluoride stands as the most suitable anion due to its small size and extraordinary electronegativity. Moreover, due to the high electronegativity of fluorine, it can delocalize π -electron density thereby forming strong hydrogen bonds which ultimately lead to the snapping of Si-O bond or deprotonation of N-H group of amide or hydroxyl group. All these factors result in the fluorometric and colourimetric detection and quantification of fluoride ions [17-24]. The binding fluoride ion lead to the origin of new emission peaks at a non-interfering wavelength which results in unambiguous detection as well as quantitative detection of fluoride ion [25]. Internal charge transfer (ICT) [26], photo-induced electron transfer (PET) [27], excited state intramolecular proton transfer (ESIPT) [28], are some of the predominant mechanisms used for chromogenic and fluorogenic chemo-sensors. Apart from these, excimer/excimer emission [29], enhancement/quenching of luminescence [30] upon fluoride attachment as well as amplification

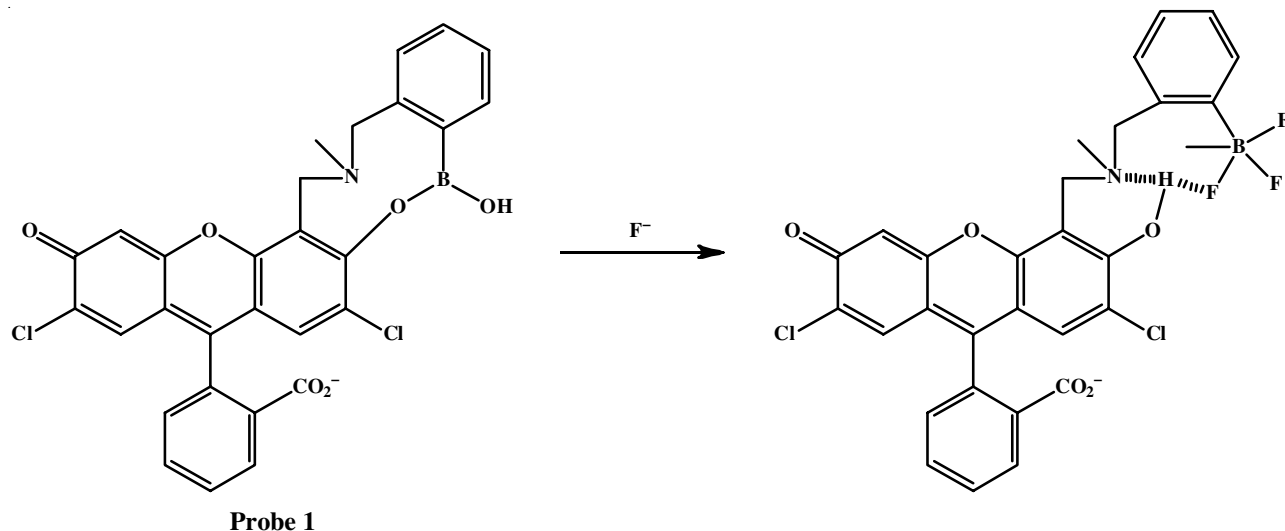


Fig. 1. A proposed mechanism for sensing F^- by **Probe 1**

of signal upon exciton-migration [31,32] are also popular mechanisms. Since fluoride is beneficial for healthy bone and teeth and at the same time detrimental if acquired in excess, detection of fluoride both qualitatively as well as quantitatively is of paramount importance [23]. In this review, we provide a compilation of various probes reported and critically analyze the advantages and disadvantages of these probes. Moreover, the principles of fluoride ion detection, designing strategies of sensors and their application in real and greener solvents have been discussed, which will be beneficial for further research in this field.

A fluorescein-based **Probe 1** principally consisting of a boronic acid group has been reported by Yoon *et al.* [34] which acts as a chemosensor for fluoride ion *via* fluorometric method showing an intense green emission in acetonitrile-methanol (9:1, v/v) (Fig. 1). When excited at 483 nm, **Probe 1** depicted a selective fluorescence “turn-on” behaviour for fluoride ion selectivity among other anions. The Cl^- ion showed minimum fluorescence enhancement with **Probe 1**, which was negligible compared to F^- ion. F^- ion selective concentration dependent fluorescence titration experiment has been performed by using 1, 10, 50, 100, 250, 500, 750 equivalent of F^- with **Probe 1** (3 μM). The association constant has been investigated as $9.2 \times 10^{10} M^{-3}$ from the fluorescence titration experiment. The mechanism may be best described by the blocking of PET mechanism through hydrogen bonding of the phenolic-H with F^- ion as well as with benzylic amine, thereby enhancing the fluorescence.

Song *et al.* [35] have introduced amino coumarin based **Probe 2** for selective F^- ion sensing with red light emission at pH 7.4, having 30% MeCN (v/v), buffered with HEPES (Fig. 2). **Probe 2** showed an absorption band with λ_{max} at 492 nm with brown colour in naked eye. When fluoride is added, the λ_{max} was found to be blue-shifted at 473 nm with concomitant colour change from brown to light brownish yellow. **Probe 2** does not show any emission in absence of fluoride ion, but shows an intense red coloured emission at 616 nm indicating the presence of fluoride ion. From the fluorescence titration spectra detection limit has been calculated and it has been found as

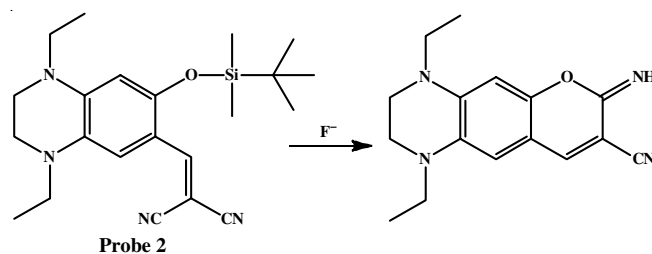


Fig. 2. A proposed mechanism for sensing F^- by **Probe 2**

$5.4 \times 10^{-6} M$. From the time dependent fluorescence study, it was found that after 10 min, saturation has achieved for **Probe 2**- F^- system. They have found a 3-fold emission enhancement after the addition of 0.01 mM F^- towards **Probe 2** (10 μM), which makes **Probe 2** as a successive tool for F^- ion detection. Interferences study has been performed using Cl^- , Br^- , I^- , CN^- , NO_3^- , HSO_4^- , AcO^- , ClO_4^- , SCN^- , N_3^- , CO_3^{2-} , *cys*, SO_4^{2-} , BSA and GSH with **Probe 2** in presence of fluoride ion, proving that **Probe 2** is applicable of detecting F^- ion selectively among other competitive anions as well as other biological analytes. The cleavage of silicon-oxygen bond of **Probe 2** and consequent cyclization imparting more rigidity in presence of fluoride ion may be regarded as responsible for the emission generated by **Probe 2**. **Probe 2** shows a stokes shift of 143 nm ($\lambda_{max,abs} = 492$ nm, $\lambda_{max,em} = 616$ nm) at pH 7.4, having 30% MeCN (v/v), buffered with HEPES, which is very much desirable for fluorescence microscopy studies. Fluorescence microscopy experiments has been performed and proved the selectivity and specificity of **Probe 2** for the identification of F^- in living HaCaT cells.

Talukdar *et al.* [36] developed a fluoride selective colourimetric and fluorescent sensors **Probe 3** (Fig. 3) had no characteristic absorption in the range 300-700 nm in DMSO, but when 300 equivalents of tetrabutylammonium fluoride (TBAF) was added to a 10 μM solution of **Probe 3** depicted a strong yellow colour, which is easily observed through naked eye. **Probe 3** exhibited a strong emission at $\lambda_{em} = 523$ nm when excited at $\lambda_{ex} = 460$ nm upon addition of fluoride ion (TBAF = 0, 0.5,

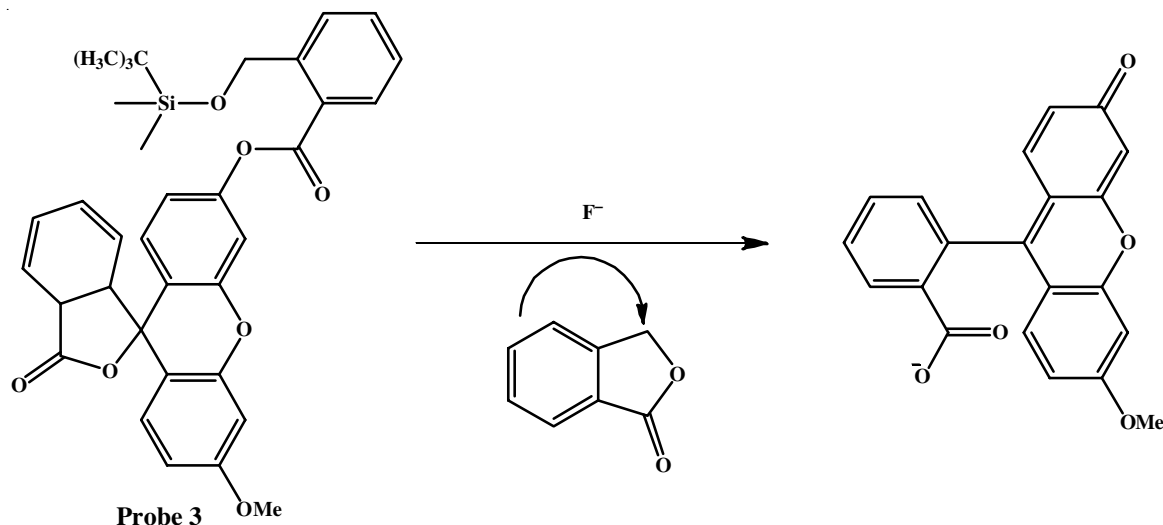


Fig. 3. A proposed mechanism for sensing F^- by **Probe 3**

1.0, 1.5, 2.0, 2.5, 3.0, 3.5 mM), thereby emitting a bright green colour. Reaction kinetics has proved the reaction to be of pseudo-first order having a rate constant $k = 0.28 \text{ min}^{-1}$ and a half-life ($t_{1/2}$) of 2.41 min. The entire sensing process took ~ 7 min to reach completion. **Probe 3** develops yellow colour through naked eye towards F^- ions and green emission colour in presence of fluoride ion under an UV-lamp. So, **Probe 3** is capable of being used successfully used for colourimetric and fluorometric detection of F^- in DMSO. The limit of detection for F^- by **Probe 3** as obtained from the experiment was $1.03 \mu\text{M}$ (19.6 ppb) much lower than 4 ppm, which is the permissible limit of F^- in drinking water as stated by the USEPA [36]. It may be mentioned here that interferences study of **Probe 3** showed selectivity towards fluoride ions among other anions (Cl^- , Br^- , I^- , ClO_4^- , NO_3^- , PF_6^- , HSO_4^- , OAc^- and SO_4^{2-}) as well as other analytes (H_2O_2 , cys and GSH) with $\lambda_{em} = 523 \text{ nm}$ when excited at $\lambda_{ex} = 460 \text{ nm}$. The mechanism of sensing was based on the cleavage of the silicon-oxygen bond of **Probe 3**, which is originally non-fluorescent. When treated with fluoride ion, it undergoes cleavage to form phthalide with consequent release of carboxy-fluorescein based fluorophore, which is the origin of yellow colour.

Zhang *et al.* [37] has reported a new chemodosimeter, **Probe 4** (Fig. 4) based on benzothiazoliumhemicyanine for selective fluorometric and colourimetric sensing of F^- in ethanol/water (30:70, v/v) solution buffered with PBS (phosphate buffer saline) (20 mM) at pH 7.4. Under this condition, **Probe 4** showed one absorption band at 407 nm, which is essentially colourless, but underwent a 110 nm red-shift with the addition of fluoride ion with an isosbestic point at 442 nm accompanied by a naked eye colour change from slight yellow to orange. Hence, **Probe 4** may be considered as useful for the identification of fluoride ion *via* “naked-eye” colour change. In the fluorescence emission spectrum λ_{em} (max) is observed at 500 nm when fluoride ion was absent, while in presence of fluoride ion, it gives a blue emission. After the addition of incremental concentrations of F^- (0, 0.5, 2, 4, 6, 10, 13, 16, 20, 24, 28, 36, 40, 50, 60 mM) with **Probe 4** (5 μM), λ_{em} is red-shifted to 558

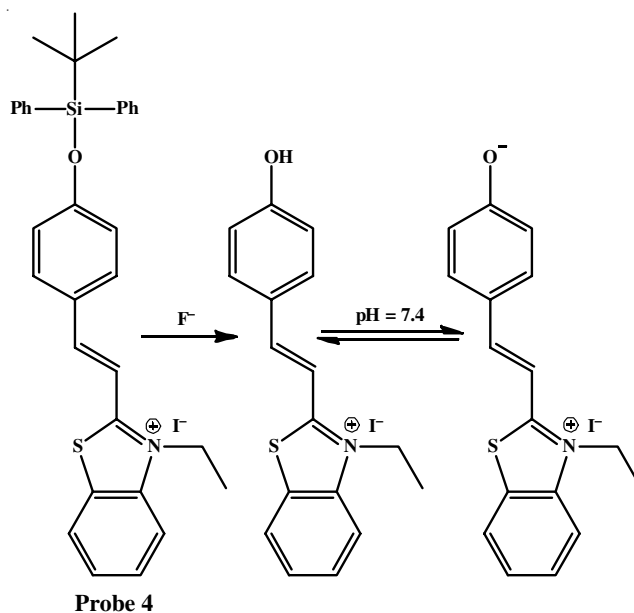
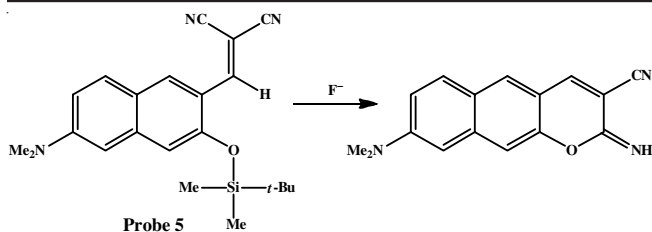
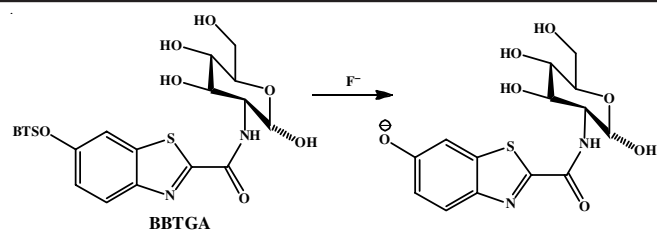


Fig. 4. A proposed mechanism for sensing F^- by **Probe 4**

nm through an iso-emission point (539 nm) resulting in the colour change from blue to green. Time dependent study has been performed and all the emission and absorption spectra were taken after 50 min. The limit of detection for F^- by **Probe 4** has been ascribed as 0.08 mM. It was found that fluoride ion detected by **Probe 4** was independent of interference by other competitive ions like Cl^- , CO_3^{2-} , Br^- , I^- , SO_4^{2-} , SCN^- , NO_3^- , N_3^- as well as other biomolecules like cysteine (cys), glutathione (GSH), bovine serum albumin (BSA) and human serum albumin (HSA). It has been found that no anions or biomolecules showed any interference for the selective detection of F^- . This selective study is based on ICT-mechanism involving fluoride ion and benzothiazolium hemicyanine dye (as fluorophore) and the mechanism is principally based on the desilylation of **Probe 4**.

Ahn *et al.* [28] reported coumarin based red light emitting fluorescent **Probe 5** (Fig. 5) for detecting the fluoride ion selectively in 20% MeCN containing 10 mM HEPES buffer

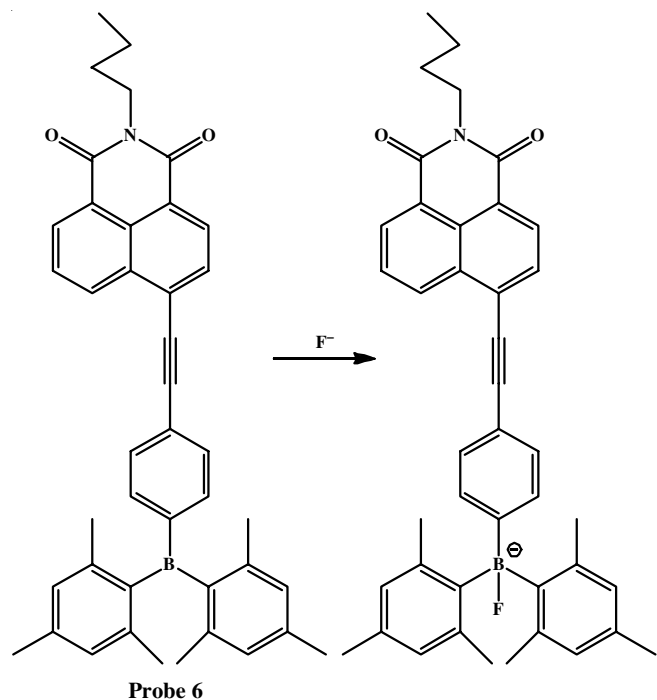
Fig. 5. A proposed mechanism for sensing F^- by **Probe 5**Fig. 6. A proposed mechanism for sensing F^- by **BBTGA**

at pH 7.4. **Probe 5** showed absorption maximum at 460 nm, which has been taken as excitation wavelength for fluorescence studies. Addition of F^- , produces no changes to absorbance of **Probe 5** and has very weak emission at 595 nm. Upon gradual addition of fluoride, more and more iminocoumarin was produced leading to the emission of more intense red light. With incremental concentration of fluoride ion (0–20 mM) towards **Probe 5** (20 μ M), the λ_{em} at 595 nm increased. From the time dependent study, it has been found that after 60 min saturation was achieved for emission study. Studies involving interference of other anions have been investigated that other anions such as Cl^- , I^- , CN^- , Br^- , HSO_4^- , NO_3^- , PF_6^- , ClO_4^- , SCN^- , CH_3COO^- , N_3^- and cysteine with **Probe 5** (20 μ M) the Si–O bond cleavage in presence of fluoride ion was not interfered by the above mentioned competing anions, even when the concentration of the anions were 10-fold higher than F^- . The highly selective fluoride ion detection was due to the fluoride-mediated desilylation process to produce red light emitting iminocoumarin, which can be showed under UV lamp. The limit of detection F^- by **Probe 5** has been estimated to be below 4 ppm, which is the permitted limit of fluoride ion in drinking water as set by USEPA. They have successfully monitored fluoride ions distribution in the three different parts of zebrafish (head, abdomen and tail parts) depending on the duration of incubation of the probe and fluoride with **Probe 5** (20 μ M and 5 mM).

Wang *et al.* [39] have reported sugar-based probe **BBTGA** (Fig. 6) as fluoride selective fluorescent sensor in (DMSO 0.5%, pH = 7.4) based on desilylation process. The sugar part has been introduced to improve the water solubility of probe **BBTGA**. **BBTGA** has very weak fluorescence, but its emission intensity has been increased by 3-fold after an incubation period of 4 h in 10 mM PBS in DMSO (0.5%) at pH = 7.4 and 5-fold after 10 h. Upon adding 0.1 M NaF to **BBTGA** in 10 mM PBS containing 0.5% DMSO at biological pH led to increase the fluorescent intensity 30 folds in 10 min at 508 nm with a green emission light. Fluorescence titration experiment has been performed by adding increasing concentration of fluoride ion (0, 0.1, 0.2, 0.3, 0.4, 0.5, 0.6, 0.7, 0.8, 0.9, 1 mM) with **BBTGA** (10 μ M). All the emission spectra were recorded after incubation time 5 min for **BBTGA** and F^- . **BBTGA** can selectively identify F^- among other competing anions by adding 0.1 M I^- , Br^- , Cl^- , F^- , $H_2PO_4^-$, NO_2^- , NO_3^- , N_3^- , AcO^- and SO_4^{2-} (total concentration 50 mM) to its solution in 10 mM PBS in 0.5%, DMSO at pH = 7.4. The selective green turn-on fluorescence of **BBTGA** in presence of F^- was achieved due to the desilylation reaction in aqueous medium. To monitor the sensitivity of **BBTGA** towards F^- ions, living cell imaging study has been done by using KB human carcinoma cell lines. This probe **BBTGA** has

proved its utility as novel fluorescence sensor by some excellent properties such as excellent interference free detection of F^- ions and fast reaction rate, in presence of other competing anions and non-cytotoxic to mammalian cells, which is essential for cellular imaging.

Misra *et al.* [40] designed and synthesized triarylborane substituted naphthalimide based **Probe 6** (Fig. 7) for selective detection of F^- by the Sonogashira cross-coupling reaction in THF solvent. **Probe 6** can selectively detect F^- and CN^- ions in the presence of myriad competing anions like NO_2^- , Cl^- , I^- , Br^- , *etc.* by turn-off method. Upon addition of increasing concentration of fluoride ion, the absorption bands at 378 and 398 nm gradually decreases with concomitant emergence of a new band at 427 nm through two isosbestic points at 304 and 407 nm, respectively. **Probe 6** (10.66 μ M) has significant emission intensity at 423 nm with blue emission light. With incremental concentration of fluoride ions to **Probe 6** in THF, the intensity of emission **Probe 6** at 423 nm decreased gradually and underwent a red-shift towards 501 nm with emission intensity quenching. The selective turn-off detection of fluoride ion by **Probe 6** has been based on the binding of F^- towards boron centre in **Probe 6**. The sensing mechanism of F^- and CN^- ions by **Probe 6** has been observed by performing DFT calculations. The theoretical calculations were in tune with the experimental

Fig. 7. A proposed mechanism for sensing F^- by **Probe 6**

findings. The computation of energy levels showed that the energy gap between the HOMO and LUMO decreased considerably upon binding with fluoride and cyanide, thereby red-shifting of absorption maxima of triarylborane substituted naphthalimide **Probe 6**.

Talukdar *et al.* [41] have reported **Probe 7** (Fig. 8) for selective detection of F^- via green fluorescence in ethanol-HEPES buffer (10 mM, pH = 7.4) solution taken in 9:1 ratio, which displayed a strong absorption centred at $\lambda_{max} = 399$ nm having a molar extinction coefficient value, $\epsilon = 12\,190\text{ M}^{-1}\text{ cm}^{-1}$. After addition of fluoride ion towards **Probe 7**, a selective yellow colour was produced, which may be due to the formation of amine derivative of **Probe 7** after the addition of F^- . **Probe 7** displayed negligible fluorescence intensity as well as a low quantum yield at 535 nm. After the addition of 0–3.5 mM of TBAF to **Probe 7** (10 μM) in 10 mM EtOH–HEPES buffer (pH = 7.4) taken in 9:1 (v/v) ratio, the fluorescence intensity at $\lambda = 535$ nm ($\lambda_{ex} = 460$ nm) increased till 60 min. Interferences study of **Probe 7** (10 μM) was carried out for F^- in the presence of many competing anions *e.g.* NO_3^- , Cl^- , Br^- , I^- , ClO_4^- , PF_6^- , OAc^- , HSO_4^- and SO_4^{2-} (2 mM) in presence with F^- (2 mM). It has been found that in presence of all competing anions, **Probe 7** can selectively and effectively detect F^- . Colourless to yellow change of colour was visible through naked eye only in the presence of the F^- ion and other anions failed to provide any colour changes. Fluorescence microscopic technique was successfully applied for live-cell imaging using the with the A549 (human lung carcinoma) cell line, which proved the cell permeability of **Probe 7** and its capability to detect intracellular F^- ions.

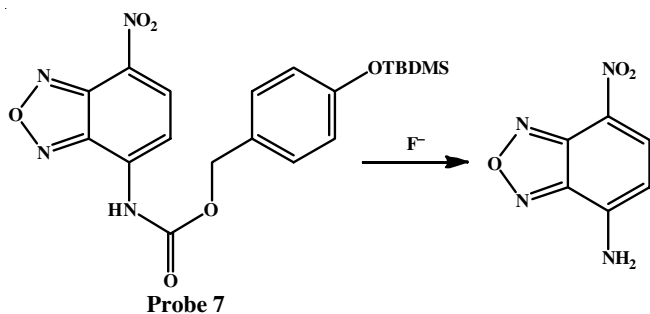


Fig. 8. A proposed mechanism for sensing F^- by **Probe 7**

Misra *et al.* [42] reported **BODIPY 4** (Fig. 9) based colourimetric and fluorescent sensors for fluoride anion detection in THF medium. The triarylborane based BODIPY can serve as highly sensitive ‘naked eye’ marker for fluoride ions with the colour changing from orange to pink. Selectivity of fluoride over other anions by **BODIPY 4** has been monitored by performing fluorescence titration using **BODIPY 4** against other competing anions *i.e.* I^- , Cl^- , Br^- and NO_3^- . It was found that **BODIPY 4** can selectively detect fluoride ion while it does not respond to other anions like Cl^- , I^- , Br^- and NO_3^- . The absorption spectra of **BODIPY 4** (10 μM) shows the significant changes with different concentrations of fluoride ions (0, 0.1, 0.2, 0.3, 0.4, 0.5, 0.6, 0.7, 0.8, 0.9, 1.0 equiv.); causes significant colour changes from orange to pink through naked eye, (a) the

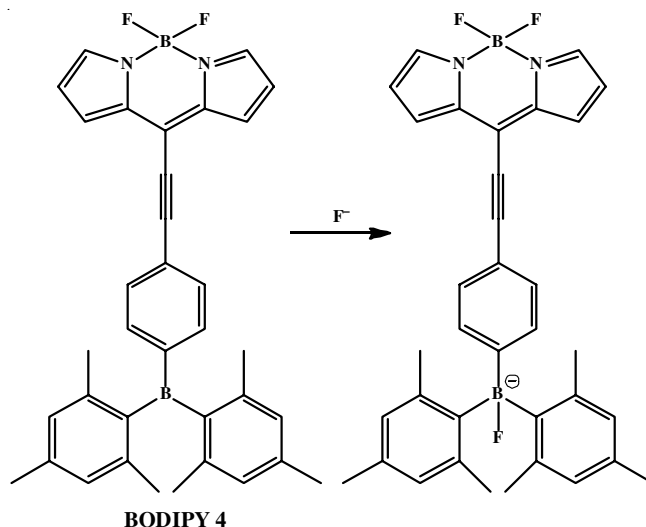


Fig. 9. A proposed mechanism for sensing F^- by **BODIPY 4**

band at 300–430 nm decreases gradually and (b) the absorption band at 547 nm experiences a blue shift of 15 nm with its intensity increasing gradually. The probable reaction mechanism of this type of absorption changes is thought to be due to the binding of fluoride ion to the trivalent boron species of **BODIPY 4** to give rise to a tetrahedral species, which decreases the degree of π -extended structure of **BODIPY 4**. Job’s plot was performed at 427 nm by absorption study and a 1:1 stoichiometry between **BODIPY 4** and fluoride ions have been found. The calculated binding constant has been investigated as $2.41 \times 10^4\text{ M}^{-1}$ for complex formation between **BODIPY 4** and F^- . Incremental concentration of F^- ion (0, 0.1, 0.2, 0.3, 0.4, 0.5, 0.6, 0.7, 0.8, 0.9, 1.0 equiv.) to the solution of **BODIPY 4** (10 μM) in THF, leads to decrease in emission intensity at 566 nm accompanied by a colour change from yellow to green under UV light.

Talukdar *et al.* [43] designed and synthesized a resorufin based colourimetric and fluorescent sensor **Probe 8** (Fig. 10), which is found to be highly selective for fluoride ion in THF medium. **Probe 8** has strong absorption bands at $\lambda = 347$ and 437 nm and was totally non-fluorescent in THF. After addition of 0.5 mM TBAF to **Probe 8** (10 μM) in THF, the peaks obtained from absorption spectra at $\lambda = 347$ and 437 nm, which decreased gradually with newly emerging absorption peaks at $\lambda = 550, 573$ and 591 nm with a strong pink colour through naked eye. These new absorption peaks are attributed to the liberated ‘free resorufin derivative’ and release of the fluoro-phore was observed to be completed after 5 min. Absorption titration experiment has been performed where the signals correspond

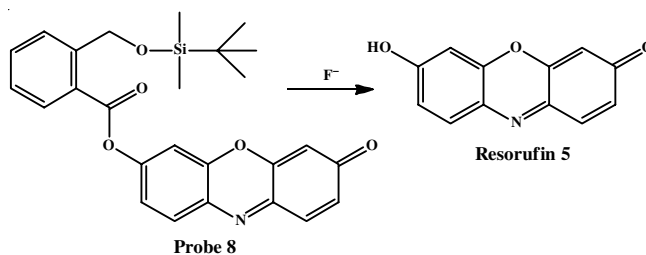
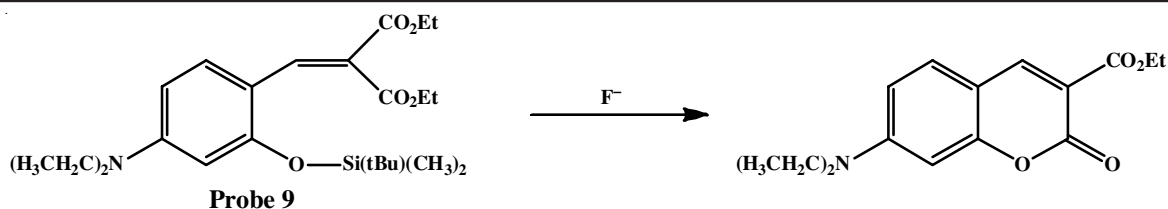


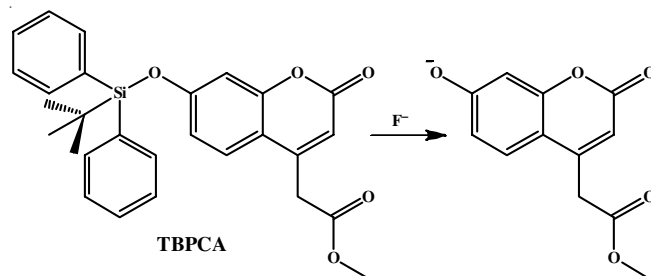
Fig. 10. A proposed mechanism for sensing F^- by **Probe 8**

Fig. 11. A proposed mechanism for sensing F^- by **Probe 9**

to **Probe 8** (at $\lambda = 347$ and 437 nm) were disappeared and signals corresponding to resorufin (at $\lambda = 550$, 573 and 591 nm) appeared. Emission titration experiment was also conducted by using **Probe 8** ($10 \mu\text{M}$) with addition of 0 – 0.7 mM F^- ion in THF ($\lambda_{\text{exc}} = 550$ nm, $\lambda_{\text{em}} = 595$ nm) and all spectra were recorded in after 10 min of mixing. After addition of F^- towards **Probe 8** in THF, red emission colour was developed. In terms of the selectivity of **Probe 8**, various interfering anions were tested in 0.5 mM of Cl^- , Br^- , I^- , PF_6^- , ClO_4^- , NO_3^- , SO_4^{2-} , HSO_4^- , OAc^- , Na_2S , H_2O_2 , cys and GSH for a span of 10 min at room temperature. None of these interfering analytes showed any significant enhancement in the emission wavelength or intensity. The detection limit has been investigated as 60 nM (1.15 ppb). For fluoride, **Probe 8** gives strong pink fluorescence and for other analytes no fluorescence was observed. The mechanism of sensing was based on fluoride anion triggered of silicon-oxygen bond cleavage in **Probe 8** and production of resorufin.

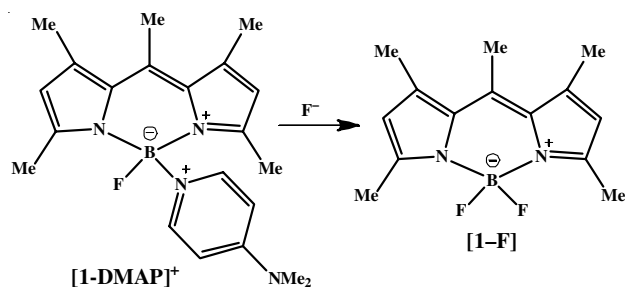
Swager & Kim [31] introduced a new system **Probe 9** (Fig. 11) with an objective of fluoride ion detection based on fluoride triggered Si-O bond cleavage and cyclization reaction, which was found to amplify the signal within a semiconducting organic polymer and the mechanism is believed to have been caused by exciton migration. In comparison to previously reported semiconductive-polymer sensor strategies that depend on the variations in emission intensity, **Probe 9** tracks a new fluorescence signal observed at 450 nm. The cyclization reaction between **Probe 9** and fluoride ion is irreversible and governed by the reaction kinetics. The fluorescence monitored the cyclization kinetics of **Probe 9** in THF concluded that it was of first-order and was independent of the concentration of fluoride ion and also relatively slow reaction takes place as the rate constant value was $2 \times 10^{-4} \text{ s}^{-1}$. The rate constants did not vary with the addition of fluoride ion in the range 0.5 to 3 molar ratio relative to **Probe 9** ($3.2 \mu\text{M}$). They have found that the silyl cleavage occurred rapidly while the cyclization was the slow step. In the fluorescence titration experiment, it has been found that there was an enhancement in the rate when a 10-fold excess of fluoride ion was added and a saturation of the emission intensity was observed after 2 h. Additional ionic associations helped acceleration of rate at the high fluoride concentrations.

Hong *et al.* [44] developed a coumarin based fluoride ion sensor **TBPCA** (Fig. 12) in HEPES buffer. With an objective to improve the water solubility and cell permeability of sensor, the hydrophilic moieties were introduced using a methyl ester group to 4-acetic acid on the fluorescent coumarin moiety. With addition of all competing anions *i.e.* Cl^- , Br^- , I^- , NO_3^- , AcO^- , N_3^- , $H_2PO_4^-$; only F^- was able to enhance the emission

Fig. 12. A proposed mechanism for sensing F^- by **TBPCA**

of **TBPCA**. The emission saturation was observed after 4 h of addition of 1 mM of NaF in HEPES buffer to $2 \mu\text{M}$ solution of **TBPCA**. Fluorescence titration experiment has been done with addition of 0 – 1.3 mM of F^- to **TBPCA** ($2 \mu\text{M}$). From the fluorescence titration experiment, emission at 461 nm was taken and linearity was achieved against concentration of F^- to **TBPCA**. The advantage of the calibration graph at 461 nm is that quantitative estimation of NaF, obtained from any sample can be easily plotted and determined. The interference study of **TBPCA** for F^- has been performed in presence of various competing anions (1 mM) such as Cl^- , Br^- , I^- , N_3^- , AcO^- , NO_3^- , $H_2PO_4^-$, *etc.* The mechanism for specific ion based turn-on fluorescence of **TBPCA** in presence of NaF may be due to the ICT mechanism and Si-O bond cleavage upon the attack of fluoride ion on the silyl ether moiety.

Hudnall & Gabbai [45] described an unique approach for the fluorescent sensing by ‘turn-on’ mechanism for F^- ions in $CHCl_3$ based on bond cleavage of **[1-DMAP]⁺** and formation of brightly fluorescent **1-F**. In this, BODIPY boronium cation (**[1-DMAP]⁺**) (Fig. 13) was treated with fluoride ion was converted to a neutral BODIPY dye (**1-F**). The neutral BODIPY dye (**1-F**) was highly fluorescent with emission colour of green. Interferences study has been done in presence of other anions like Cl^- , I^- , Br^- and it was found there were no any significant emission enhancement from other anions. After addition of 1 equiv. of TBAF, the fluorescence intensity has increased by a factor of 500% and the emission colour can be easily observed with

Fig. 13. A proposed mechanism for sensing F^- by **[1-DMAP]⁺**

naked eye. In presence of iodide ions, the cationic *p*-dimethylaminopyridine adduct of 1,3,5,7,8-pentamethylpyrrometheneboron fluoride [**1-DMAP**]⁺ reacts with fluoride ions to produce the corresponding brightly fluorescent **1-F**.

Manez *et al.* [46] used a silica matrix to impregnate the **Probe 10** (Fig. 14) to detect the presence of fluoride ion in real samples. The solvent used was acetonitrile-water (7:3, v/v) buffered with 0.1 M potassium hydrogen phthalate and HCl, maintaining a pH of 2.5. **Probe 10** gives pink colour which can be seen by naked eye, which makes this probe as an excellent colourimetric tool for fluoride anion. Large surface area (*ca.* 1000 m² g⁻¹) of the probe allows a high degree of functionalization which, in turn, will be translated to a higher response of the final solid. At the same time, the MCM-41 silica porous system may provide proper protection for the signalling molecules. **Probe 10** can develop a significant pink colour in presence of 0.5×10^{-6} M fluoride. In order to support their approach, they have successfully applied their method for the quantitative determination of fluoride in the commercial toothpaste and a very good correlation with the claimed concentration has been found.

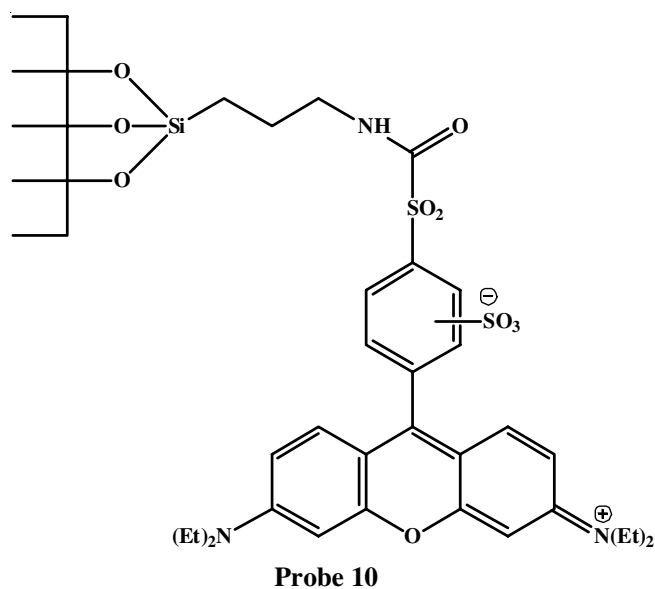


Fig. 14. Structure of **Probe 10**

Bermejo *et al.* [47] introduced **Probe 11**, which possesses two thiourea-containing unsaturated side chains connected to

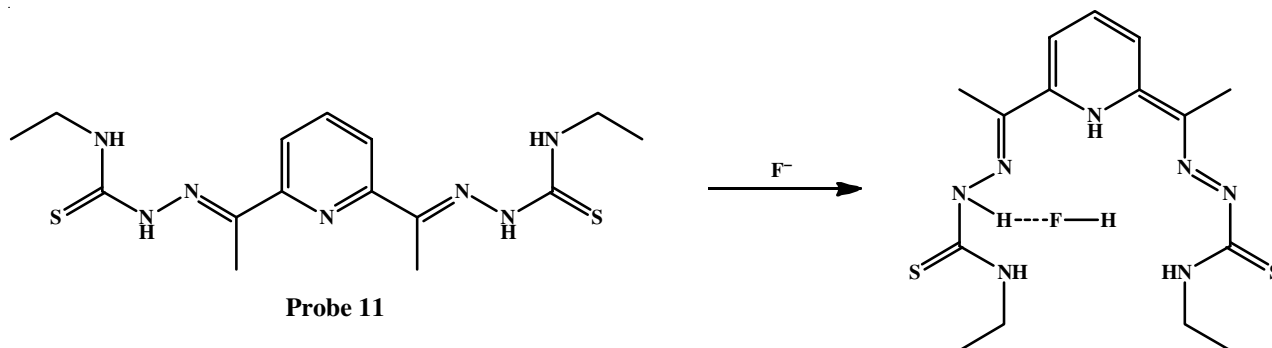
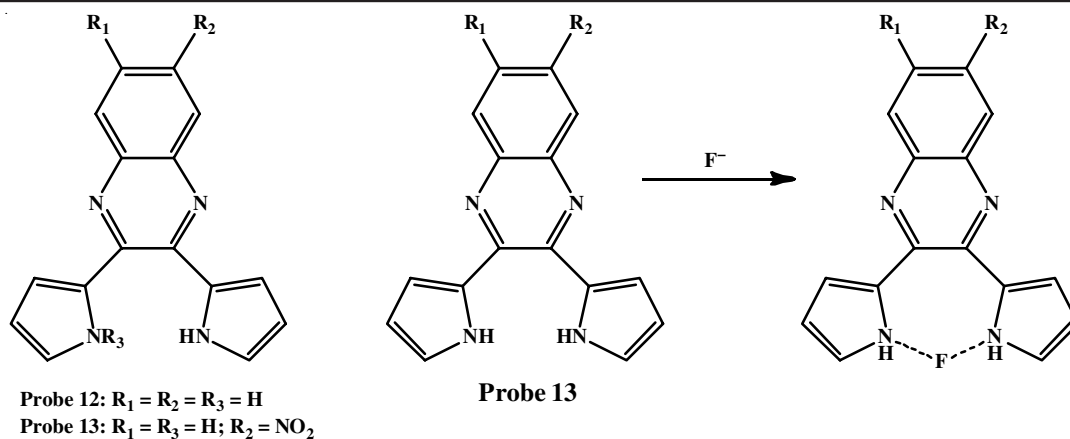


Fig. 15. A proposed mechanism for sensing F⁻ by **Probe 11**

a central pyridine ring (Fig. 15) and enabled the naked-eye detection of fluoride ions without any particular chromophore in acetonitrile. The interference study of **Probe 11** (10 μM) with several anions *i.e.* Cl⁻, Br⁻, I⁻, AcO⁻, HSO₄⁻ have been studied by the spectrophotometric titrations in acetonitrile by addition of a tetraalkylammonium salt of the competing anions to a solution of **Probe 11**. It has been showed that addition of F⁻ salt resulted in decreasing the peak at 324 nm with the emergence of a new band at 412 nm. In the absorbance titration, it has been showed that with the addition of different concentrations of F⁻ to **Probe 11**, the absorbance band at 412 nm increased gradually. The presence of an isosbestic point at 345 nm proved the presence of two species at equilibrium: **Probe 11** and a **Probe 11-F** adduct. The interaction of the thiourea-hydrogen atoms with the fluoride ion enhanced the π-delocalization and shifted the π-π* transition from the UV to the visible region and produced yellow colour. Enhanced π-delocalization on the organic backbone was expected to reduce the energy of the π-π* transition. As a result, the absorption band was shifted from the UV to the visible region and a yellow colour appeared. The visual aspects of fluoride ion recognition and sensing by **Probe 11** have been monitored by using a 10⁻⁴ M solution of **Probe 11** in MeCN. Addition of one equivalent of F⁻ ions to **Probe 11** (10 μM) induced the appearance of a bright yellow colour while the addition of 10 equiv. of the other competing anions *i.e.* Cl⁻, Br⁻, AcO⁻, I⁻, HSO₄⁻ did not induce any notable colour development.

Sessler *et al.* [48] developed dipyrrole systems (**Probes 12 and 13**) (Fig. 16) for F⁻ ion detection using UV-visible absorption methods in dichloromethane and DMSO solvents. **Probe 13** has developed fluoride anion-induced dramatic colour change from yellow to purple. In both solvents, the colour changes were reversed upon addition of water. This was due to the water molecule which competes for F⁻ at the pyrrolic-NH donating sites through hydrogen bonding. The unique sensitivity of **Probe 13** compared to **Probe 12** was may be due to the greater electron deficiency of the mononitro derivative (**Probe 13**) lead to an increase in its hydrogen bond-donating character. The diketone-2 derivative of **Probe 13** have relatively large extinction coefficient but did not fluorescence. Diketone-2 was brightly coloured in dichloromethane solution and like **Probe 12**, undergoes a naked-eye colour changes from yellow-green to orange, in presence of F⁻. The binding constant of **Probes 12 and 13** for F⁻ was investigated using fluorescence

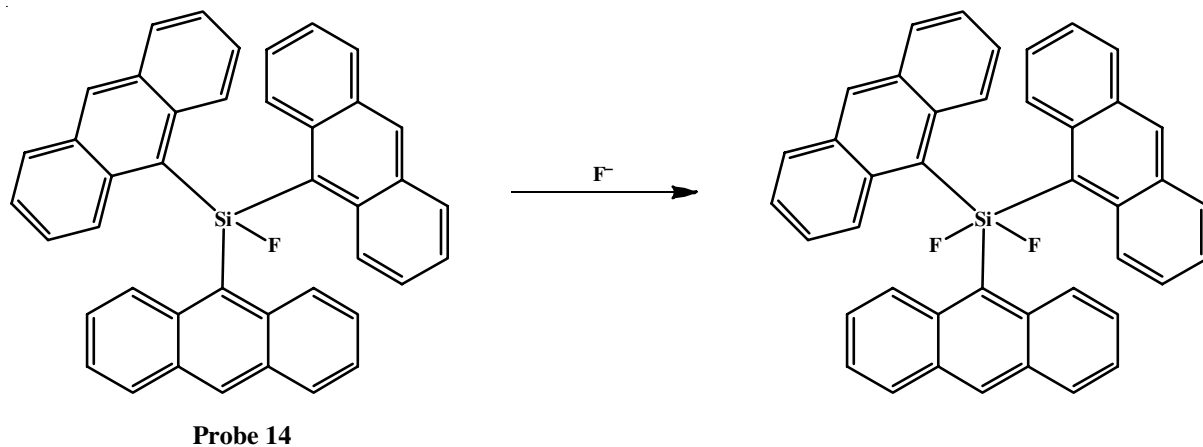
Fig. 16. A proposed mechanism for sensing F^- by **Probe 13**

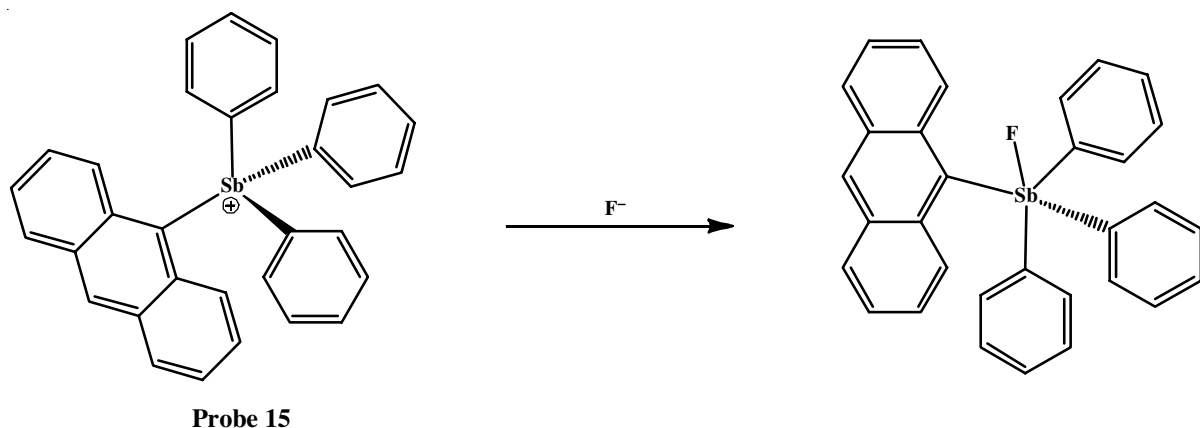
quenching data at 490 and 600 nm, respectively. It has been found that the binding constant of **Probes 12** and **13** for F^- was $18200 M^{-1}$ and $118000 M^{-1}$, respectively. The sensing mechanism was due to the presence of two pyrrole $-NH$ groups in **Probes 12** and **13** that functioned as anion binding sites and a built-in quinoxaline ring that served as a colourimetric reporter.

Tamao *et al.* [49] also reported a new type of trianthryl-fluorosilane based sensor **Probe 14** (Fig. 17) with a remarkable changes in the UV-visible absorption and fluorescence spectra in the presence of TBAF in THF solution. **Probe 14** showed absorption maximum at 401 nm. In the UV-visible absorption titration spectra, with the addition of increasing concentration of TBAF (0, 6.9, 14, 21, 27, 34, 41, 51, 62 μM) to **Probe 14** (40 μM), new bands appears at about 9 nm shorter wavelengths relative to **Probe 14** at 392 nm, along with the disappearance of the absorption bands of **Probe 14**. Fluorescence titration experiment has also been investigated adding increasing concentration of TBAF (0, 1.7, 3.4, 5.1, 6.9, 8.6, 10, 12 μM) to **Probe 14** (0.2 μM). In the fluorescence titration spectra, the emission intensity was significantly increased with about 20 nm hypsochromic shifts of the emission maxima from 416 nm to 396 nm. The “off-on” behaviour of anthryl fluorophore was controlled on the basis of coordination number of the silicon atom. In the interferences study, when other competing anionic species such as Cl^- , Br^- , I^- , ClO_4^- and BF_4^- as their $n-Bu_4N^+$ salts were added

to the silane **Probe 14**, no changes were observed both in the UV-visible absorption and fluorescence spectra. The sensing mechanism was the decrease in the degree of through-space interaction between the anthryl groups by the structural change from tetrahedral **Probe 14** to trigonal bipyramidal **Probe 14-F**, as observed in the crystal structures.

Gabbai *et al.* [50] also developed another new fluorescent sensor **Probe 15** based on 9-anthryltriphenylstibonium cation (Fig. 18) for fluoride anion in aqueous DMSO solution. **Probe 15** was found to be meagrely fluorescent, with an emission band at 427 nm which is essentially anthryl-based. Conversion of [**Probe 15**]OTf into **Probe 15-F** by addition of TBAF resulting in a blue shift of the absorption band that was principally anthryl-based, accompanied by a drastic increase in the fluorescence intensity of the anthryl fluorophore. Up to pH 5, [**Probe 15**]OTf exists as the free cation as justified by UV-vis spectroscopy. Above this pH, a distinct blue shift in the UV-Vis spectrum was observed, suggesting a binding of hydroxide anion to the antimony center. All these studies indicated that **Probe 15-OTf** served as an efficient fluoride anion sensor, predominantly at slightly acidic pH. Emission titration experiment has been carried out in 9:1 (v/v) $H_2O/DMSO$ (CTAB, 10 mM) at pH 4.8 (pyridine buffer, 10 mM) indicated that [**Probe 15**]OTf binds fluoride anion with a binding constant of $12000 \pm 1100 M^{-1}$, which can be used for the detection of fluoride in ppm. Inter-

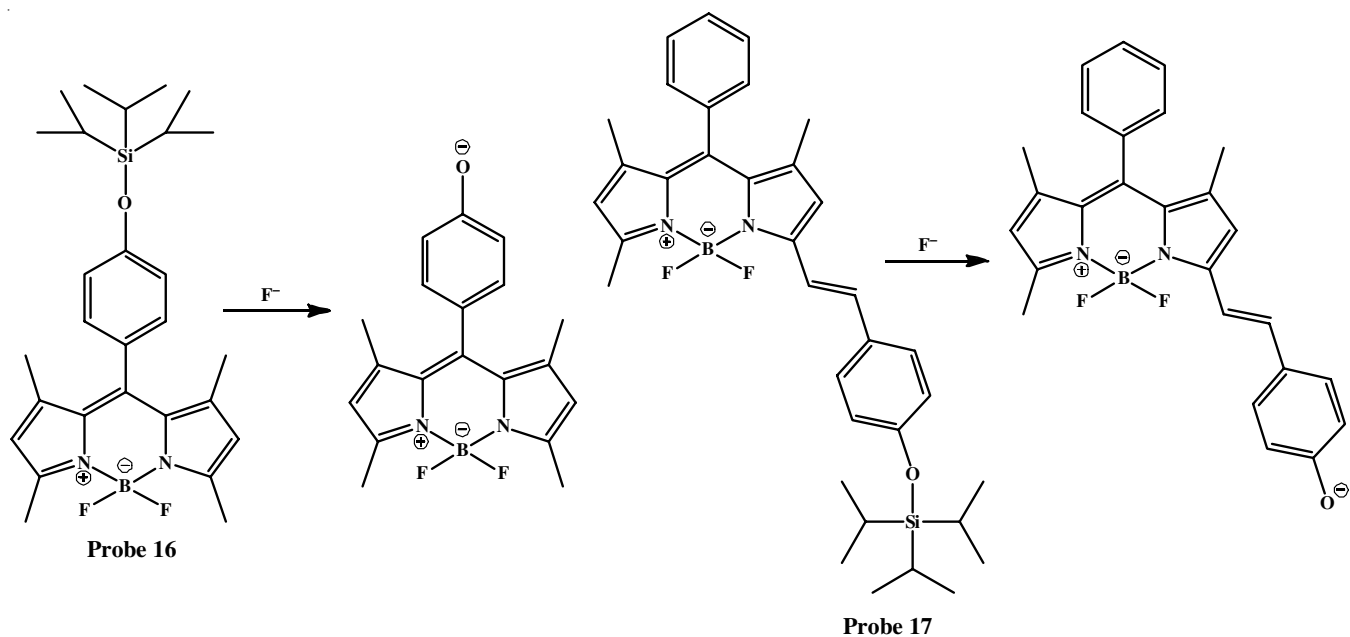
Fig. 17. A proposed mechanism for sensing F^- by **Probe 14**

Fig. 18. A proposed mechanism for sensing F^- by **Probe 15**

ference study was performed in presence of other anions such as Cl^- , I^- , Br^- , NO_3^- , HCO_3^- , N_3^- and HSO_4^- and found no interferences. They have performed fluoride ion sensitivity test by tap water as sample and bottled water. The fluorescence turn-on response was observed with the naked eye within 1 min for concentrations of at least 1 ppm.

Akkaya *et al.* [51] developed colourimetric and fluorometric sensors based on BODIPY (**Probes 16** and **17**) for fluoride in acetonitrile solution (Fig. 19). **Probe 16** has the absorption maximum at 498 nm. In the absorption titration experiment, with the addition of increasing concentration of fluoride ions (0, 0.025, 0.05, 0.075, 0.1, 0.125, 0.15, 0.2, 0.25, 0.375, 0.5 mM) in the form of a tetrabutylammonium salt to solution of **Probe 16** ($5 \mu M$), resulted changes of 10 nm blue shift to the absorption spectrum. In the emission titration of **Probe 16** ($5 \mu M$), the emission at 506 nm was quenched by a factor of 20 in the presence of increasing concentration of fluoride ions (0, 0.025, 0.05, 0.075, 0.1, 0.125, 0.15, 0.2, 0.25, 0.375, 0.5 mM). In the absorption titration experiment, **Probe**

17 ($5 \mu M$) showed a large bathochromic shift on addition of increasing concentration of fluoride ions (0, 0.025, 0.05, 0.075, 0.1, 0.125, 0.15, 0.2, 0.25 mM). The absorption peak at 560 nm gradually decreased and a new peak at 682 nm emerged with an isosbestic point at 581 nm. Red shift of 120 nm in absorption was a remarkable change in solution and corresponds to a colour change from purple to green. In the emission titration spectrum of **Probe 17** ($5 \mu M$), the emission was quenched in the presence of increasing concentration of fluoride ions (0, 0.025, 0.05, 0.075, 0.1, 0.125, 0.15, 0.2, 0.25 mM). **Probes 16** and **17** can selectively detect F^- which has been visualized by the naked eye colour and emission colour under UV lamp. All the spectra were recorded for **Probes 16** and **17** with F^- after few seconds and 5 min of mixing respectively. Interference study has been performed for **Probe 16** ($5 \mu M$) and **Probe 17** ($5 \mu M$) in presence of F^- with other competitive anions *i.e.* Cl^- , I^- , Br^- , CN^- , AcO^- , NO_3^- , $H_2PO_4^-$, HSO_4^- (0.5 mM and 0.25 mM, respectively) and it was found that no any anions gave any interference during the detection of F^- . The plausible mechanism for the

Fig. 19. A proposed mechanism for sensing F^- by **Probe 16** and **Probe 17**

unique sensitivity was due to the silicon-oxygen bond cleavage facilitated by fluoride anions and generated strong intramolecular charge transfer (ICT) from donor phenoxide ion in complete conjugation with BODIPY dye and resulted in a significant red shift in the absorbance spectra.

Lee *et al.* [52] developed a *tris*(*N*-salicylideneamine)-derived 'turn-on' fluorescent sensor (**Probe 18**, Fig. 20) for fluoride anion through covalently triggered conformational switching mechanism in dichloromethane solvent. A cleavable silyl-ether groups was introduced to a dynamic fluorophore system for structural unfolding and fluorescence quenching. After the addition of increasing concentration of fluoride ion, desilylation process was occurred which triggered spontaneous structural folding and the recovery of an intense blue emission originating from a planar conjugated *tris*(*N*-salicylideneaniline) motif. In CH_2Cl_2 , **Probe 19** displays intense visible absorptions at 420 and 440 nm. Upon excitation at 340 nm, **Probe 19** emits at 458 nm which reflects the rigid molecular structure. The mechanism of fluorescence turn-on in this system was based

exclusively on the Si-O bond cleavage reactions of **Probe 18**. The interferences study of **Probe 18** ($5 \mu\text{M}$) for F^- against Cl^- , CN^- , Br^- , I^- , ClO_4^- , SCN^- , NO_3^- , HSO_4^- , PF_6^- and H_2PO_4^- anions ($50 \mu\text{M}$) has been investigated. Only F^- among the competing anions generated measurable increase in the fluorescence signal, whereas Cl^- , CN^- , Br^- , I^- , SCN^- , HSO_4^- , NO_3^- , PF_6^- , ClO_4^- and H_2PO_4^- had no effect under similar conditions.

Kim & Hong [53] reported dosimeter based on resorufin (**Probe 20**, Fig. 21) for selective fluoride anion detection *via* colourimetric and fluorometric method in 1:1 (v/v) acetonitrile-water as well as in acetonitrile. With the addition of F^- in different concentrations induced decrease in the absorption maximum of **Probe 20** at $20 \mu\text{M}$ at 445 nm and increase at 586 nm in acetonitrile with naked-eye colour change from pale yellow to pink. Other anions did not cause any change in absorption spectra as well as in naked eye colour. **Probe 20** depicted an eye-catching change in UV-vis absorption and fluorescence emission by fluoride addition as compared to other anions in acetonitrile as well as in acetonitrile-water mixture (1:1, v/v).

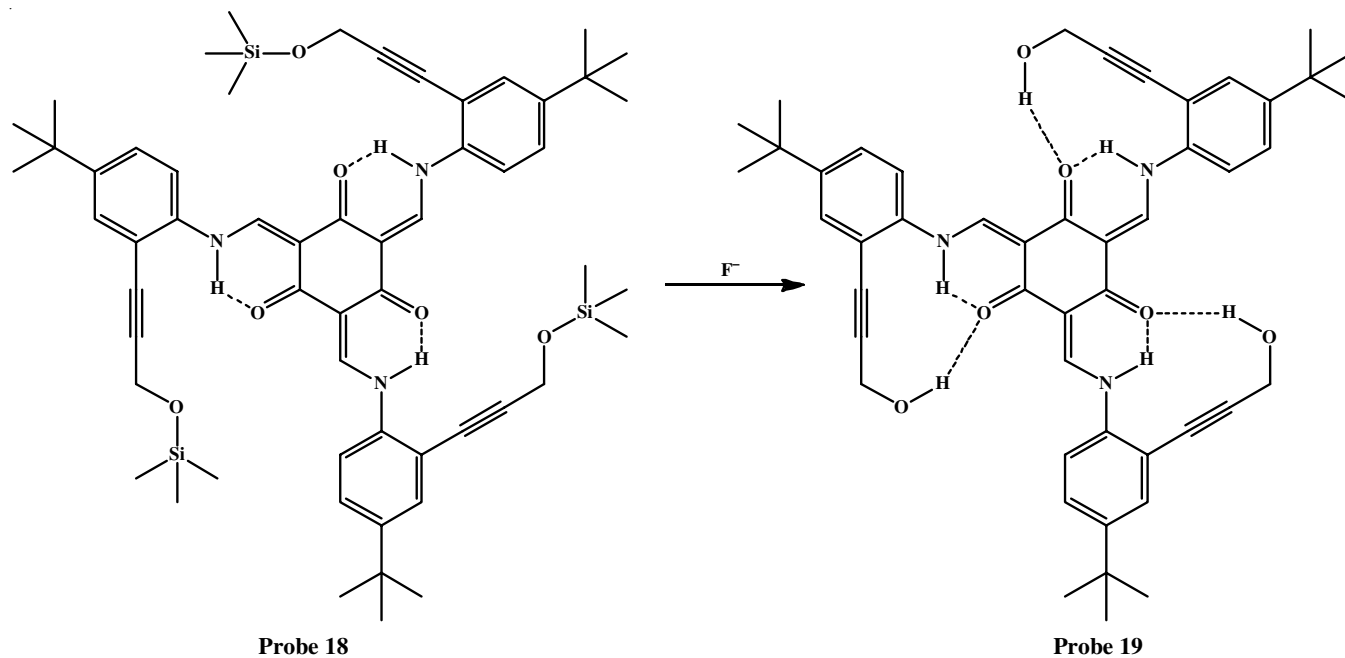


Fig. 20. A proposed mechanism for sensing F^- by **Probe 18**

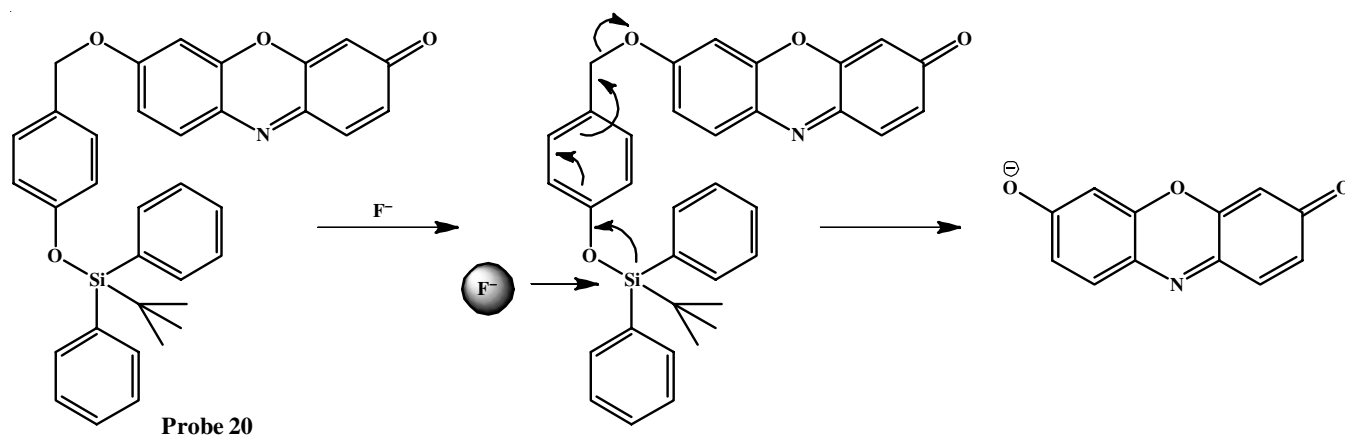


Fig. 21. A proposed mechanism for sensing F^- by **Probe 20**

Fluorescence emission titration experiment of **Probe 20** (5 μM) with increasing concentration of F^- at 591 nm ($\lambda_{\text{ex}} = 550$ nm) has been examined in acetonitrile. In presence of F^- in different concentrations, the emission intensity of **Probe 20** increased by 500-folds at 591 nm and saturated at 1400 equivalents of F^- . Over time, the colour changed from pale yellow to pink. Upon addition of TBAF (5 mM) to **Probe 20** (5 μM) also depicted a large enhancement of emission in 1:1 MeCN/ H_2O solution. The possible mechanism for such remarkable colour change and enhancement in emission was attributed to fluoride induced silicon-oxygen bond cleavage that resulted in the formation of a highly fluorescent resorufin.

To summarize, this review describes various colourimetric and fluorometric sensors for fluoride ions in aqueous medium as well as mixed solvents. Some important characteristics of these sensors are mentioned in Table-1. The remarkable parameters like working solvent system, limit of detection, wave length changes with naked-eye colour and emission colour changes and their application in real samples and cell imaging are also summarized.

Since in the ratiometric approach, the wavelength is generated at a different wavelength hence this method is also useful in the unambiguous determination of fluoride ion. Hence, the ratiometric approach is extremely popular among

TABLE-1
COMPARISON OF IMPORTANT FEATURES OF REPORTED FLUORIDE ION SENSORS

Probe	End point	Solvent	Detection time	Detection limit	Mechanism	Applications	Ref.
Probe 1	Fluorometric changes from light green to bright green	Acetonitrile-MeOH (9:1, v/v)	n.d.	n.d.	Inhibition of PET process and hydrogen bonding	–	[34]
Probe 2	Fluorometric changes from light green to bright green and colorimetrically from brown to brownish yellow	HEPES buffer (pH = 7.4, containing 30% CH_3CN , v/v)	10 min	5.4×10^{-6} M	F-triggered Si–O bond cleavage Probe 2 and a subsequent rigidizing, cyclization reaction	Living HaCaT cells	[35]
Probe 3	Fluorometric changes from light green to bright green and colorimetrically	DMSO	7 min	1.03 μM (19.6 ppb)	Cleavage of the Si–O bond of Probe 3 and release of carboxy fluorescein-based fluorophor	Living cells (HeLa cells)	[36]
Probe 4	Fluorometric changes from slight yellow to orange and colorimetrically from blue to green	Ethanol and water (3:7, v/v) solution containing phosphate buffered saline (PBS) (20 mM, pH 7.4)	50 min	0.08 mM	ICT-mechanism between Probe 4 and F- and the cleavage of Si-O bond in Probe 4	RAW 264.7 macrophage living cells	[37]
Probe 5	Fluorometric changes from colorless to bright red	HEPES buffer solution (10 mM, pH 7.4) containing acetonitrile (20% by volume)	60 min	Below 4 ppm	Fluoride-mediated desilylation process to produce iminocoumarin	Zebrafish (head, abdomen, and tail parts)	[38]
BBTGA	Fluorometric changes from colorless to green	PBS (phosphate buffered saline) (DMSO 0.5%, pH = 7.4)	5 min	n.d.	Fluoride-mediated desilylation process	KB human carcinoma cell lines	[39]
Probe 6	Fluorometric changes from blue to light blue	THF	n.d.	2.01×10^{-10} M	Binding of F- towards the Boron centre of Probe 6	–	[40]
Probe 7	Fluorometric changes from blue to green and colorimetrically from colorless to yellow	(9:1) ethanol-HEPES buffer (10 mM, pH = 7.4) solution	60 min	n.d.	Fluoride-mediated desilylation process and production of ammine derivative of Probe 7	A549 (human lung carcinoma) cell line	[41]
BODIPY 4	Fluorometric changes from yellow to green and colorimetrically from orange to pink	THF medium	n.d.	n.d.	Photoinduced electron transfer process from BODIPY to trivalent boron	–	[42]
Probe 8	Fluorometric changes from colorless to red and colorimetrically from yellow to pink	THF	5 min	60 nM (i.e. 1.15 ppb)	Fluoride-mediated desilylation process and production of resorufin	HeLa cell line	[43]
Probe 9	Fluorometric changes from colorless to blue	THF	2 h	n.d.	Fluoride triggered Si-O bond cleavage and formation of a highly fluorescent coumarin through cyclization reaction	–	[31]
TBPCA	Fluorometric changes from colorless to blue	HEPES buffer (water)	4 h	n.d.	ICT mechanism and Si-O bond cleavage upon the attack of fluoride ion on the silyl ether moiety	A549, human epithelial lung carcinoma cell	[44]
[1-DMAP]⁺	Fluorometric changes from light green to bright green	CHCl_3	n.d.	n.d.	bond cleavage of [1-DMAP] ⁺ and formation of brightly fluorescent 1-F	–	[45]

Probe 10	Colorimetric changes from colorless to pink	Acetonitrile:water (7:3) (v/v) solutions buffered to pH = 2.5 with 0.1 M potassium hydrogenphthalate and HCl acid	n.d.	n.d.	–	Commercial toothpaste	[46]
Probe 11	Colorimetric changes from colorless to yellow	Acetonitrile	n.d.	n.d.	The interaction of the thiourea-hydrogen atoms with the fluoride ion via hydrogen bonding	–	[47]
Probe 13	Colorimetric changes from yellow to purple for Probe 13	Dichloromethane and DMSO	n.d.	n.d.	Hydrogen bonding between pyrrole NH groups of Probe 12 and Probe 13 and F ⁻	–	[48]
Probe 14	Fluorometric changes from light blue to bright blue	THF	n.d.	n.d.	Decrease in the degree of the through-space interaction between the anthryl groups by the structural change from tetrahedral Probe 14 to trigonal bipyramidal Probe 14-F	–	[49]
Probe 15	Fluorometric changes from light blue to bright blue	DMSO	n.d.	0.38 ppm	Structural change from tetrahedral Probe 15 to trigonal bipyramidal Probe 15-F	Tap water sample (College Station, TX) and bottled water (Evian, France)	[50]
Probe 16	Colorimetrically from yellow to brown	Acetonitrile	5 min	n.d.	Si-O bond cleavage facilitated by fluoride anions will generate strong intramolecular charge transfer (ICT)	(PMMA) films impregnated with Probe 16 and Probe 17	[51]
Probe 17	Colorimetrically from purple to green						
Probe 18	Fluorometric changes from light blue to bright blue	CH ₂ Cl ₂	n.d.	n.d.	Si-O bond cleavage reactions of Probe 18 and hydrogen bonding	–	[52]
Probe 20	Fluorometric changes from colorless to red and colorimetrically from pale yellow to pink	CH ₃ CN/H ₂ O (50:50, v/v), CH ₃ CN	3 min	n.d.	Fluoride-triggered Si-O bond cleavage that results in the formation of a highly fluorescent resorufin	–	[53]

n.d. = not detected

researchers, so far as fluoride ion detection and quantification is concerned. Sahana & Dutta [54] had thoroughly discussed the ratiometric approach in a recent critical review and hence, this review is dedicated to the discussion of the merits and demerits of colourimetric and fluorometric sensors only.

Comparative study of the fluoride sensing Probes

Detection time: From the above table, it is evident that **Probe 20** is most efficient with a detection time of 3 min. A close peer of **Probe 20** is **Probe 8** with a detection time of 5 min. Both these probes contain the resorufin moiety which is principally responsible for a very quick detection of fluoride ion. Similarly, **BBTGA**, **Probe 16** and **Probe 17** also possess a quick detection time 5 min although **Probe 16** and **Probe 17** comprise of **BODIPY** moiety while **BBTGA** contain benzothiazole as the active fluorophore. Hence, all these 5 probes may be considered as equally effective so far as the detection time is concerned and the choice for applicability of these probes has to be determined by comparing the other parameters.

Detection limit: Among the studied sensors, **Probe 6** has a detection limit of 2.01×10^{-10} M of fluoride ion, while its closest competitor is **Probe 8** with a detection limit of 60 nM. Rest of the probes have much lower detection limit typically ranging in micro-molar concentration of fluoride ion.

Water solubility: **TBPCA** is unique among all the probes because of its functioning in aqueous medium (HEPES buffer). The increased water solubility is due to the incorporation of

4-acetic acid group with methyl tagged coumarin. This side chain not only increases the cell permeability of the active fluorophore but also enhances its retainivity of the fluorophore within the cell because of the negatively charged carboxylate group, thereby providing a better insight of the sensor mechanism of association of the fluorophore with fluoride ion within the cell.

Probe 5 stands next to **TBPCA** for its applicability in aqueous medium as its working solvent is found to be water: acetonitrile (80:20, v/v) in HEPES buffer, while **Probe 2** is close to **Probe 5** with its applicability in water:acetonitrile (70:30, v/v) in HEPES buffer. It may be mentioned here that with coumarin based fluorophores, the water solubility is found to be increased and hence coumarin may be considered as the fluorophore of choice for designing sensors that can work effectively for water soluble fluoride samples.

However, there is no unique probe which can be singled out as the best sensor for fluoride ion detection as each one of them has some merits on one parameter, while the other has better quality on a different parameter. For example, while **TBPCA** is applicable in aqueous medium, **Probe 20** has the minimum detection time of 3 min and **Probe 6** has the lowest detection limit of 2.01×10^{-10} M of fluoride ion. It will be intriguing for future researchers to design sensors for fluoride ion detection with optimized value of all the parameters like time of detection, detection limit *vis-a-vis* its applicability in applicability in aqueous medium.

Conclusion

This review article provides an overview of the many viewpoints on the colorimetric and fluorescent sensors for the detection and measurement of fluoride ions among other competing anions in water or other solvents as well as the research conducted on their potential uses. Discussion regarding the working solvent system, limit of detection, association constant, time required for sensing, studies involving interference of other anions, mechanism of sensing, sensing properties and their applications in the real samples as well as biological samples. Fluoride ions specific changes in the wavelength as observed by naked eye and emission/fluorescence colour changes are also thoroughly discussed. The principal mechanisms that have been utilized for fluoride ion sensing namely silicon-oxygen bond cleavage, formation of monomer boron-fluorine bond, deprotonation of amide bond by means of strong H \cdots F hydrogen bonding, silicon-fluorine bond formation and antimony-fluorine bond formations are also extensively discussed. Strategic designing of the probes *vis-a-vis* their advantages and disadvantages so far as the various parameters are concerned, with respect to detection and identification of fluoride ion in water and biological samples have also been critically analyzed. The use of chromophores like benzothiazoliumhemicyanine, naphthalimide, benzothiazole, benzoxadiazole, thiourea, rhodamine, BODIPY, fluorescein, coumarine, resorufin, anthracene derivatives possessing huge importance as colourimetric and fluorescent sensors, as well as disease-related study in cells have been discussed in this review. A critical analysis of the probes in view of their use in aqueous medium and possible ways to improve their solubility in water or water-based medium have also been discussed. It is hopeful that the concepts regarding the principles of fluoride ion detection and explanations of the observations that have been discussed in this review article would further enhance the ability of future researchers to design colourimetric and fluorescent probes for the qualitative and quantitative determination of fluoride anion with increased selectivity and to realize their mechanism of sensing, solvent dependency, wavelength or colour changes as well as their applications in therapeutic usage.

ACKNOWLEDGEMENTS

The authors are thankful to The Principal, Nistarini College, Purulia, India for all kinds of research support. The authors are also thankful to Prof. Debasis Das, Department of Chemistry, The University of Burdwan, Burdwan and Dr. Papu Biswas, Associate Prof., Department of Chemistry, Indian Institute of Engineering Science and Technology, Shibpur, India for their constant encouragement and support.

CONFLICT OF INTEREST

The authors declare that there is no conflict of interests regarding the publication of this article.

REFERENCES

- D. Wu, A.C. Sedgwick, T. Gunnlaugsson, E.U. Akkaya, J. Yoon and T.D. James, *Chem. Soc. Rev.*, **46**, 7105 (2017); <https://doi.org/10.1039/C7CS00240H>
- J. Chan, S.C. Dodani and C.J. Chang, *Nat. Chem.*, **4**, 973 (2012); <https://doi.org/10.1038/nchem.1500>
- Z. Guo, S. Park, J. Yoon and I. Shin, *Chem. Soc. Rev.*, **43**, 16 (2014); <https://doi.org/10.1039/C3CS60271K>
- L. You, D. Zha and E.V. Anslyn, *Chem. Rev.*, **115**, 7840 (2015); <https://doi.org/10.1021/cr5005524>
- H. Zhu, J. Fan, B. Wang and X. Peng, *Chem. Soc. Rev.*, **44**, 4337 (2015); <https://doi.org/10.1039/C4CS00285G>
- Z. Yang, A. Sharma, J. Qi, X. Peng, D.Y. Lee, R. Hu, D. Lin, J. Qu and J.S. Kim, *Chem. Soc. Rev.*, **45**, 4651 (2016); <https://doi.org/10.1039/C5CS00875A>
- J. Li, D. Yim, W.D. Jang and J. Yoon, *Chem. Soc. Rev.*, **46**, 2437 (2017); <https://doi.org/10.1039/C6CS00619A>
- S. Singha, D. Kim, H. Seo, S.W. Cho and K.H. Ahn, *Chem. Soc. Rev.*, **44**, 4367 (2015); <https://doi.org/10.1039/C4CS00328D>
- J. Yan, S. Lee, A. Zhang and J. Yoon, *Chem. Soc. Rev.*, **47**, 6900 (2018); <https://doi.org/10.1039/C7CS00841D>
- J.W. Steed and J.L. Atwood, *Supramolecular Chemistry*, Wiley: Hoboken, edn. 2 (2009).
- Z. Wang, H. Luecke, N. Yao and F.A. Quioco, *Nat. Struct. Biol.*, **4**, 519 (1997); <https://doi.org/10.1038/nsb0797-519>
- J.W. Pflugrath and F.A. Quioco, *Nature*, **314**, 257 (1985); <https://doi.org/10.1038/314257a0>
- C. Caltagirone and P.A. Gale, *Chem. Soc. Rev.*, **38**, 520 (2009); <https://doi.org/10.1039/B806422A>
- A.F. Li, J.H. Wang, F. Wang and Y.B. Jiang, *Chem. Soc. Rev.*, **39**, 3729 (2010); <https://doi.org/10.1039/b926160p>
- P.A. Gale, *Chem. Soc. Rev.*, **39**, 3746 (2010); <https://doi.org/10.1039/c001871f>
- P.A. Gale, *Chem. Commun.*, **4525**, 4525 (2008); <https://doi.org/10.1039/b809508f>
- M.E. Moragues, R. Martinez-Manez and F. Sancenon, *Chem. Soc. Rev.*, **40**, 2593 (2011); <https://doi.org/10.1039/c0cs00015a>
- M. Li, Z. Liu, H. Wang, A.C. Sedgwick, J.E. Gardiner, S.D. Bull, H.N. Xiao and T.D. James, *Dyes Pigments*, **149**, 669 (2018); <https://doi.org/10.1016/j.dyepig.2017.11.033>
- X. Wu, X.X. Chen, B.N. Song, Y.J. Huang, W.J. Ouyang, Z. Li, T.D. James and Y.B. Jiang, *Chem. Commun.*, **50**, 13987 (2014); <https://doi.org/10.1039/C4CC04542D>
- T. Nishimura, S.Y. Xu, Y.B. Jiang, J.S. Fossey, K. Sakurai, S.D. Bull and T.D. James, *Chem. Commun.*, **49**, 478 (2013); <https://doi.org/10.1039/C2CC36107H>
- S.J.M. Koskela, T.M. Fyles and T.D. James, *Chem. Commun.*, 945 (2005); <https://doi.org/10.1039/b415522j>
- C.M. López-Alled, A. Sanchez-Fernandez, K.J. Edler, A.C. Sedgwick, S.D. Bull, C.L. McMullin, G. Kociok-Köhn, T.D. James, J. Wenk and S.E. Lewis, *Chem. Commun.*, **53**, 12580 (2017); <https://doi.org/10.1039/C7CC07416F>
- M. Li, G.E.M. Lewis, T.D. James, Y.T. Long, B. Kasprzyk-Hordern, J.M. Mitchels and F. Marken, *ChemElectroChem*, **1**, 1640 (2014); <https://doi.org/10.1002/celec.201402181>
- V. Amendola, D. Esteban-Gómez, L. Fabbrizzi and M. Licchelli, *Acc. Chem. Res.*, **39**, 343 (2006); <https://doi.org/10.1021/ar0501951>
- B.L. Schottel, H.T. Chifotides and K.R. Dunbar, *Chem. Soc. Rev.*, **37**, 68 (2008); <https://doi.org/10.1039/B614208G>
- V. Thiagarajan, P. Ramamurthy, D. Thirumalai and V.T. Ramakrishnan, *Org. Lett.*, **7**, 657 (2005); <https://doi.org/10.1021/ol047463k>
- E.B. Veale and T. Gunnlaugsson, *J. Org. Chem.*, **73**, 8073 (2008); <https://doi.org/10.1021/jo8012594>
- Y. Wu, X. Peng, J. Fan, S. Gao, M. Tian, J. Zhao and S. Sun, *J. Org. Chem.*, **72**, 62 (2007); <https://doi.org/10.1021/jo061634c>
- S.K. Kim, J.H. Bok, R.A. Bartsch, J.Y. Lee and J.S. Kim, *Org. Lett.*, **7**, 4839 (2005); <https://doi.org/10.1021/ol051609d>

30. R. Martínez-Máñez and F. Sancenón, *Chem. Rev.*, **103**, 4419 (2003); <https://doi.org/10.1021/cr010421e>
31. T.H. Kim and T.M. Swager, *Angew. Chem. Int. Ed.*, **42**, 4803 (2003); <https://doi.org/10.1002/anie.200352075>
32. T.H. Kim and T.M. Swager, *Angew. Chem.*, **115**, 4951 (2003); <https://doi.org/10.1002/ange.200352075>
33. R.M. Duke, E.B. Veale, F.M. Pfeffer, P.E. Kruger and T. Gunnlaugsson, *Chem. Soc. Rev.*, **39**, 3936 (2010); <https://doi.org/10.1039/b910560n>
34. K.M.K. Swamy, Y.J. Lee, H.N. Lee, J. Chun, Y. Kim, S.J. Kim and J. Yoon, *J. Org. Chem.*, **71**, 8626 (2006); <https://doi.org/10.1021/jo061429x>
35. P. Hou, S. Chen, H. Wang, J. Wang, K. Voitchovsky and X. Song, *Chem. Commun.*, **50**, 320 (2014); <https://doi.org/10.1039/C3CC46630B>
36. A. Roy, D. Kand, T. Saha and P. Talukdar, *Chem. Commun.*, **50**, 5510 (2014); <https://doi.org/10.1039/c4cc01665c>
37. B. Zhu, F. Yuan, R. Li, Y. Li, Q. Wei, Z. Ma, B. Du and X. Zhang, *Chem. Commun.*, **47**, 7098 (2011); <https://doi.org/10.1039/c1cc11308a>
38. D. Kim, S. Singha, T. Wang, E. Seo, J.H. Lee, S.J. Lee, K.H. Kim and K.H. Ahn, *Chem. Commun.*, **48**, 10243 (2012); <https://doi.org/10.1039/c2cc35668f>
39. B. Ke, W. Chen, N. Ni, Y. Cheng, C. Dai, H. Dinh and B. Wang, *Chem. Commun.*, **49**, 2494 (2013); <https://doi.org/10.1039/C2CC37270C>
40. T. Sheshashena Reddy, R. Maragani and R. Misra, *Dalton Trans.*, **45**, 2549 (2016); <https://doi.org/10.1039/C5DT04039F>
41. A. Roy, A. Datar, D. Kand, T. Saha and P. Talukdar, *Org. Biomol. Chem.*, **12**, 2143 (2014); <https://doi.org/10.1039/c3ob41886c>
42. R. Misra, T. Jadhav, B. Dhokale and S.M. Mobin, *Dalton Trans.*, **44**, 16052 (2015); <https://doi.org/10.1039/C5DT02356D>
43. A. Roy, D. Kand, T. Saha and P. Talukdar, *RSC Adv.*, **4**, 33890 (2014); <https://doi.org/10.1039/C4RA06933A>
44. S.Y. Kim, J. Park, M. Koh, S.B. Park and J.I. Hong, *Chem. Commun.*, **4735–4737**, 4735 (2009); <https://doi.org/10.1039/b908745a>
45. T.W. Hudnall and F.P. Gabbai, *Chem. Commun.*, **4596–4597**, 4596 (2008); <https://doi.org/10.1039/b808740g>
46. A.B. Descalzo, D. Jiménez, J.E. Haskouri, D. Beltrán, P. Amorós, M.D. Marcos, R. Martínez-Máñez and J. Soto, *Chem. Commun.*, **562–563**, 562 (2002); <https://doi.org/10.1039/b111128k>
47. M. Vázquez, L. Fabbri, A. Taglietti, R.M. Pedrido, A.M. González-Noya and M.R. Bermejo, *Angew. Chem. Int. Ed.*, **43**, 1962 (2004); <https://doi.org/10.1002/anie.200353148>
48. C.B. Black, B. Andrioletti, A.C. Try, C. Ruiperez and J.L. Sessler, *J. Am. Chem. Soc.*, **121**, 10438 (1999); <https://doi.org/10.1021/ja992579a>
49. S. Yamaguchi, S. Akiyama and K. Tamao, *J. Am. Chem. Soc.*, **122**, 6793 (2000); <https://doi.org/10.1021/ja001042q>
50. I.S. Ke, M. Myahkostupov, F.N. Castellano and F.P. Gabbai, *J. Am. Chem. Soc.*, **134**, 15309 (2012); <https://doi.org/10.1021/ja308194w>
51. O.A. Bozdemir, F. Sozmen, O. Buyukcakir, R. Guliyev, Y. Cakmak and E.U. Akkaya, *Org. Lett.*, **12**, 1400 (2010); <https://doi.org/10.1021/ol100172w>
52. X. Jiang, M.C. Vieweger, J.C. Bollinger, B. Dragnea and D. Lee, *Org. Lett.*, **9**, 3579 (2007); <https://doi.org/10.1021/ol7014187>
53. S.Y. Kim and J.I. Hong, *Org. Lett.*, **9**, 3109 (2007); <https://doi.org/10.1021/ol0711873>
54. S. Dutta and A. Sahana, *Anal. Methods*, **16**, 344 (2024); <https://doi.org/10.1039/D3AY01840G>